

We LHR2 09

Application of Image Consistent Time-strain Analysis to the 4D Baobab Data

H. Hoesber* (CGG), A. Khalil (CGG), S. de Pierrepont (CGG), Z. Dobo (CGG), H. Neal (CGG), C. Purcell (CGG), K. Ubik (CGG), B. Singh (CNR) & Y. Singh (CNR)

SUMMARY

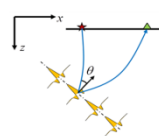
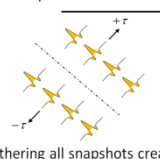
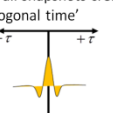
Time-lapse (4D) inversions deal with changes in seismic amplitudes and travel-times. This analysis is performed on migrated seismic images, which represent the spatial and time-lapse variability of the medium's reflectivity. 4D reservoir analysis methods such as inversion and warping need to follow the structure of the data. Migration effectively rotates the wavelet so that it is normal to the imaged reflectors; however, the 1D (vertical) convolutional approach, commonly used in 4D inversions to date, does not honour this directivity. For this reason we recently introduced a wave equation based method which provides an effective platform for image consistent reservoir analysis. This must be used in processes such as wavelet extraction, inversion, warping and 4D time-strain inversion. In this paper, we show a data example from the 4D Baobab survey, offshore Côte d'Ivoire, comparing warping results for time-shifts and time-strains with a 1D convolutional and the new image consistent inversion.

Introduction

A migrated seismic image represents the spatial variability of the earth's reflectivity. Imaging algorithms (migration) map the energy recorded on the surface back to the subsurface locations which generated the reflections. The migrated seismic image is then generally interpreted as the convolution of a seismic wavelet, ideally temporally and spatially constant, and the underlying reflectivity. However, the process of migration effectively rotates the seismic wavelet so that it is everywhere normal to the imaged reflectors, instead of being aligned along the time axis as in pre-migration data. For this reason, 1D convolutional based methods, whether in 3D or in a time-lapse setting, are not optimal for seismic data with more than one dip (e.g. Thore et al. 2012 and Audebert and Agut 2014). In this paper, we present an imaging based solution to this problem. Using the 4D Baobab survey, offshore Côte d'Ivoire, we compare warping results for time-shifts and time-strains with a 1D convolutional and the new image consistent inversion.

Method

In order to overcome the limitations of the 1D convolutional model after migration, we could attempt a pre-imaging approach such as 4D full waveform inversion, as proposed by Asnaashari et al. (2011). This is computationally expensive but worthy of investigation. Our solution, which we call "image consistent", instead continues to operate on depth-migrated data (Khalil and Hoeber 2016, Khalil et al. 2015a, 2015b). Briefly put (see inset), we reintroduced the concept of seismic image waves, originally proposed by Hubral et al. (1996), to define an image domain wave equation. At each depth location

<p>1. A seismic image of a common angle is viewed as a snapshot of a propagating wave-field at zero time.</p> 	<p>3. We find the solution at earlier and later snapshots.</p> 
<p>2. This wave-field is governed by a wave equation</p> $\frac{1}{v^2(\mathbf{x})} \partial_t^2 I(\mathbf{x}; \tau) = \nabla^2 I(\mathbf{x}; \tau);$ $v(\mathbf{x}) = \frac{1}{2} \frac{c(\mathbf{x})}{\cos(\theta)}$	<p>4. Gathering all snapshots creates a new axis: 'orthogonal time'</p> 

this equation generates a series of images propagated in accordance with the local structure. This new axis, which we call "orthogonal time", allows us to perform kinematic and amplitude inversions of depth imaged seismic data with dipping and complex structures. The method is applicable to pre- and poststack data and is easily combined with existing inversion and warping tools, as we may now use 1D convolutional methods along the orthogonal time axis. For

example, in order to determine the time-shift or time-strain between base and monitor at a certain location (x,y) and (z=depth), we propagate both vintages, imaged with the same velocity model, along orthogonal time at that location, using the local imaging velocity. We can then apply any existing warping or inversion algorithm along this new axis. An intuitive way to understand this procedure is to consider it as the answer to the following question: Given the base, how much more or how much less do we have to propagate the monitor to achieve optimal 4D time-alignment? Once the time-shift and time-strain are determined, they are posted to the un-propagated location (x,y,z) in depth and can be displayed and inspected as before.

Baobab example, offshore Côte d'Ivoire

The processing area under consideration covers the Baobab field, offshore Côte d'Ivoire. Water depths vary from approximately 760m to 1650m with pronounced canyons developing off the shallow water shelf area. The structure is a 4-way dip closure formed by the Late Albian unconformity and extensional faulting. The reservoir has been subdivided into several stratigraphical units on the basis of prominent seismic reflectors. These units have tabular geometry. The Middle to Late Albian (Lower Cretaceous) reservoir succession comprises dominantly fine to medium grained thin turbidite sandstones interbedded with siltstones and mudstones deposited in a restricted syn-rift seaway between the West African Craton and the East Brazilian Microplate. A complex history of uplift, erosion and subsequent sedimentation created a complex overburden, imposing major challenges for seismic imaging of the reservoir interval. In addition, approximately 25% of the field area is affected by poor imaging due to a number of gas clouds. The two seismic vintages are from 1999 and 2014.

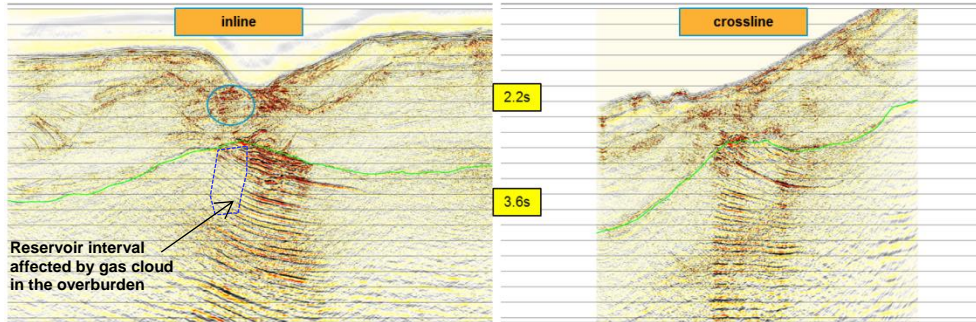


Figure 1 4D differences prior to warping. The gas cloud zone is indicated with a blue circle on the inline. Top reservoir horizon is shown in green.

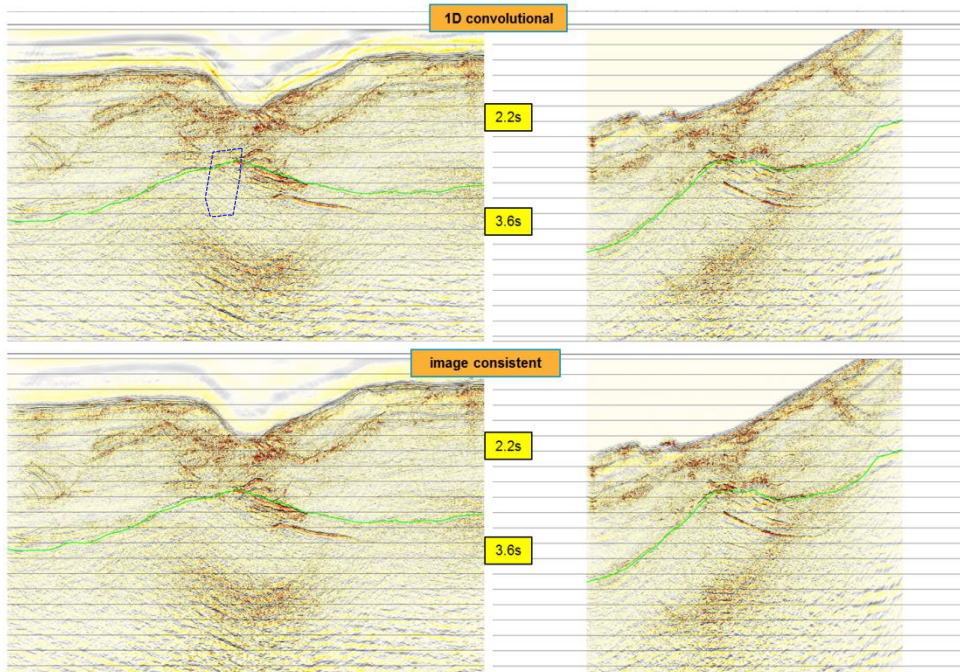


Figure 2 4D differences after warping with conventional (top 2 images) and image consistent warping. Both methods achieve very comparable results.

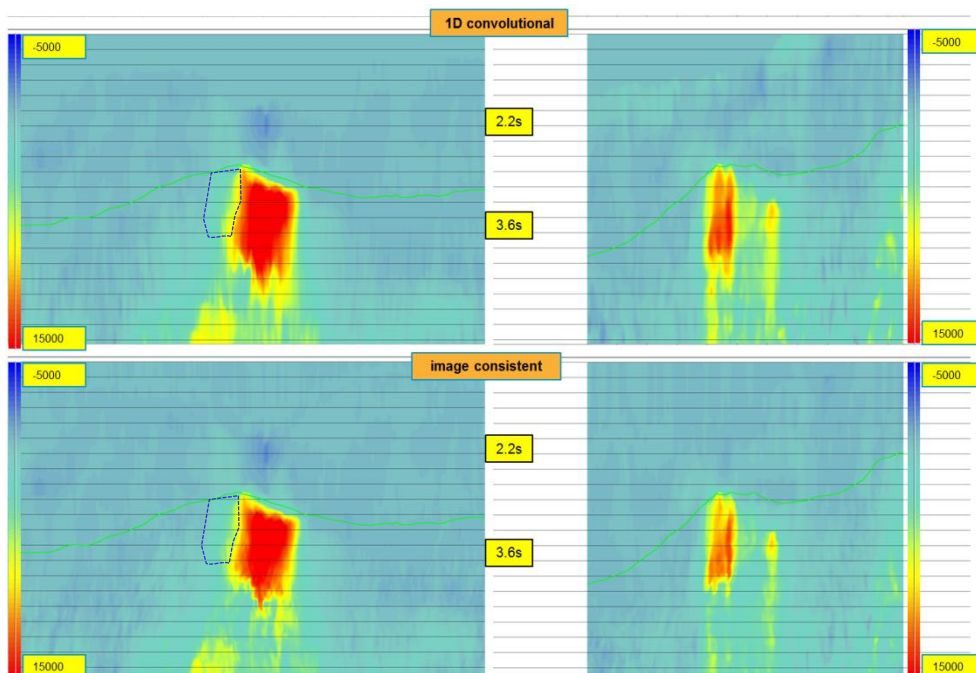


Figure 3 Time-shifts [μ s] with conventional and image consistent warping. We see only minor differences.

Careful 4D processing with regular 4D quality checks was carried out in 2015. The main 4D objectives in the context of the analysis shown here were: tracking the oil-water contact and identifying bypassed zones and areas of low injection support. Processing challenges were in particular: water velocity changes, overburden changes due to gas, and spectral differences in the data due to different acquisitions. Processing steps to address these challenges included updating the background velocity model with two passes of multi-layer tomography and modelling the gas bodies using a combination of FWI, seismic interpretation and velocity scanning. Despite the challenges, the final depth-imaged post-stack data that we use in the following time-strain analysis was deemed of high quality except in the areas affected by the gas clouds.

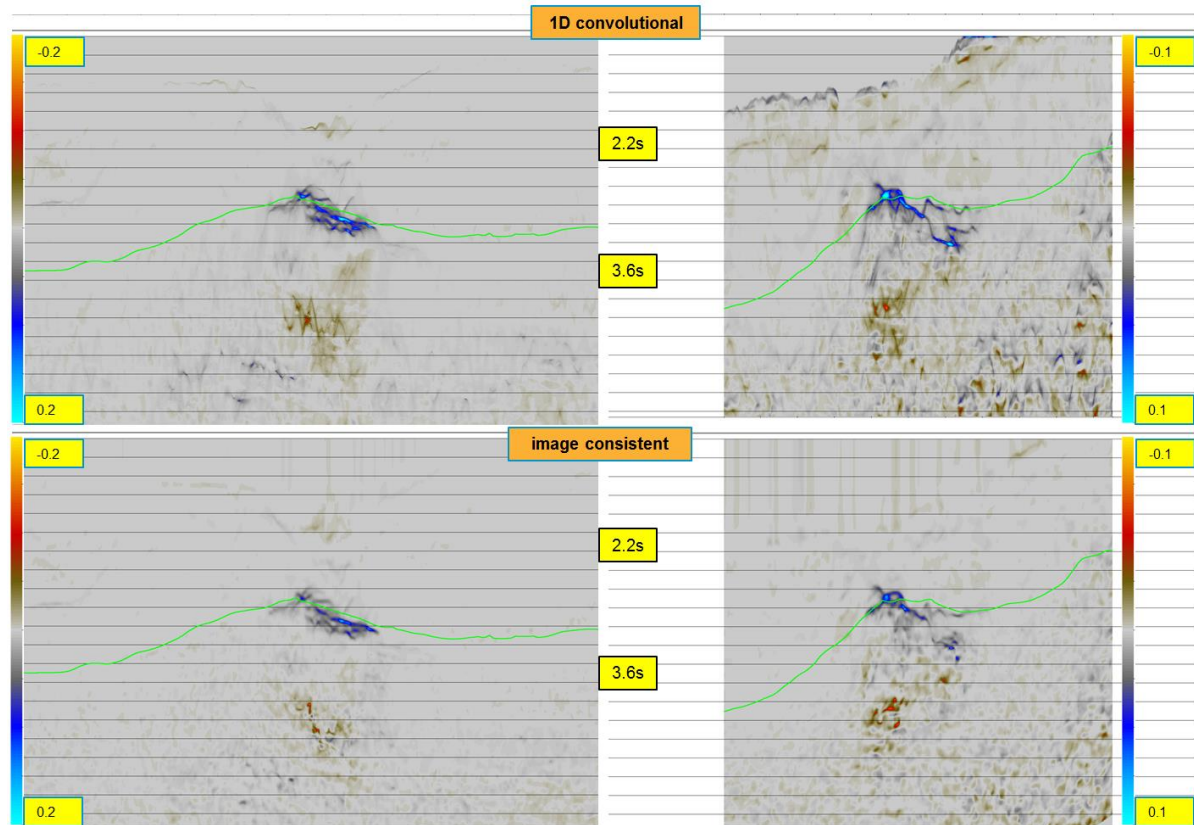


Figure 4 Time-strains obtained with the 1D (top 2 images) and the image consistent warping. Image consistent warping is less noisy, more geologically consistent and has higher vertical resolution.

Figure 1 shows two different views of “raw” 4D differences prior to any warping. The green horizon delineates the top of the reservoir. Figures 2 and 3 repeat the same section views as in Figure 1, showing 4D differences after warping, and time-shift attributes. Results are shown for the 1D convolutional method (top two section displays in each quadrant) and the image consistent warping (bottom two section displays). In both cases, warping was computed by a basic cross-correlation method, with suitable outlier detection after the attribute calculation.

Comparing results in Figure 2 we see little, if any, differences by eye in the 4D difference sections. Time-shift attributes are also very comparable, as is often the case with the different warping and time-shift algorithms. Comparing time-strains however (the time derivatives of the time-shifts), we see several effects (Figure 4). Firstly, the image consistent time-strain warping is overall cleaner. This is true at the high frequencies, and the 1D convolutional time-strain also has some small low frequency noise visible – we attribute this to the dip-dependent stretch effects. Secondly, we see some footprint effects when using the 1D convolutional method, mostly to the right-hand side of the 4D effects. This is absent when using the image consistent warping approach.

Figure 5 is a zoom of the two time-strain results around the reservoir area. This shows again that the image consistent warping is less noisy, and also has higher vertical resolution. We have verified these

results using a variety of alternative warping engines, including non-linear inversions with Tikhonov smoothness or layer constraints, and we find the observations to be independent of the algorithm used.

Conclusions

The 1D convolutional approach has served us well and is still used today in most reservoir inversion engines. Its underlying assumption, of a dip independent wavelet is, however, false. The real data example from the 4D Baobab shows that an image consistent warping method yields a cleaner, higher resolution, and more geologically consistent time-strain attribute than the 1D convolutional method. Future work will look at coupling the time-strain inversion to the amplitude inversion.

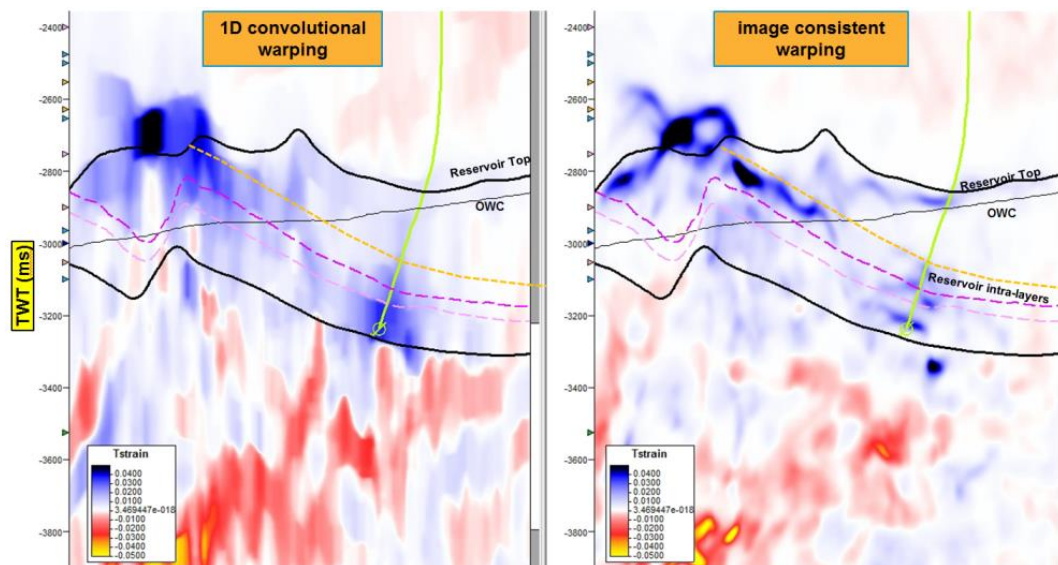


Figure 5 Zoom of the time-strains for a crossline at an injector. Image consistent time-strains are less noisy, have higher vertical resolution and are more geologically consistent.

Acknowledgments

The authors thank CNR International (UK) Ltd., Svenska Petroleum Exploration CI AB and Petroci Holding, Côte d'Ivoire, as well as CGG management, for permission to publish this work.

References

- Asnaashari, A., Garambois, S., Audebert, F., Thore, P., and Virieux, J. [2011] Sensitivity analysis of time-lapse images, *81st Annual International Meeting, SEG*, Expanded Abstracts.
- Audebert, F., and Agut, C. [2014] Making time-domain warping applicable to the retrieval of 4D perturbations. *84th Annual International Meeting, SEG*, Expanded Abstracts.
- Hubral, P., Tygel, M., and Schleicher, J. [1996] Seismic image waves. *Geophysical Journal International*, **125**, pp. 431-442.
- Khalil, A. and Hoerber, H. [2016] Wave-equation based image warping. *Geophysics*, Vol. **81**(1), pp V1-V6.
- Khalil, A., Hoerber, H., Deschizeaux, B. and Campbell, S. [2015a] Spectral Analysis of post imaging seismic data. *77th Annual International Conference and Exhibition, EAGE*, Extended Abstracts.
- Khalil, A., Hoerber, H., Jafargandomi, A. and de Pierrepont, S. [2015b] Wavefield driven reservoir analysis. *77th Annual International Conference and Exhibition, EAGE*, Extended Abstracts.
- Thore, P., de Verdier, C. and McManus, E. [2012] Estimation of 4D signal in complex media, A fast track approach. *82nd Annual International Meeting, SEG*, Expanded Abstracts.